Analytical solutions of nonlocal Poisson dielectric models with multiple point charges inside a dielectric sphere

Dexuan Xie,[*] Hans W. Volkmer, and Jinyong Ying

Department of Mathematical Sciences, University of Wisconsin-Milwaukee, Milwaukee, Wisconsin 53201-0413, USA

The nonlocal dielectric approach has led to new models and solvers for predicting electrostatics of proteins (or other biomolecules), but how to validate and compare them remains a challenge. To promote such a study, in this paper, two typical nonlocal dielectric models are revisited. Their analytical solutions are then found in the expressions of simple series for a dielectric sphere containing any number of point charges. As a special case, the analytical solution of the corresponding Poisson dielectric model is also derived in simple series, which significantly improves the well known Kirkwood's double series expansion. Furthermore, a convolution of one nonlocal dielectric solution with a commonly used nonlocal kernel function is obtained, along with the reaction parts of these local and nonlocal solutions. To turn these new series solutions into a valuable research tool, they are programed as a free FORTRAN software package, which can input point charge data directly from a protein data bank file. Consequently, different validation tests can be quickly done on different proteins. Finally, a test example for a protein with 488 atomic charges is reported to demonstrate the differences between the local and nonlocal models as well as the importance of using the reaction parts to develop local and nonlocal dielectric solvers.

I. INTRODUCTION

The nonlocal dielectric approach has been studied for more than 30 years for the purpose of improving the quality of the classic Poisson dielectric approach [1–8]. It features a position-dependent dielectric permittivity function over the whole space to reflect either the polarization correlations of water molecules or the spatial-frequency dependence of a dielectric medium. However, such a permittivity function results in a partial derivative-mixed convolution term, making a nonlocal dielectric model become very difficult to study.

The early study was done mainly on a Lorentz nonlocal model with a dielectric sphere containing one central point charge or the charge near a half-space [9,10]. The case of a dielectric sphere containing multiple charges was studied with an approximate method [11,12]. To sharply reduce the complexity of solving the Lorentz nonlocal model, Hildebrandt *et al.* modified the Lorentz nonlocal model into a system of coupled partial differential equations (PDEs) [13]. From this system of coupled PDEs, they obtained an analytical solution for the case of a dielectric sphere with one central point charge [13]. Using this PDE system, recently, Bardhan *et al.* [14] found the analytical solution for a dielectric sphere containing multiple point charges as a double series in terms of the surface spherical harmonics of boundary-integral operators. However, they did not report any coefficient of the series. Since the PDE system of Hildebrandt *et al.* is an approximation to the Lorentz nonlocal model, the analytical solution of the Lorentz nonlocal model with D_p containing multiple charges was still unknown so far.

Motivated by the novel work of Hildebrandt *et al.*, a fast finite element algorithm for solving a Lorentz nonlocal model for water was developed in [15]. This Lorentz nonlocal model was then extended into a nonlocal Poisson dielectric model for a protein in an ionic solvent [16]. Recently, a nonlocal modified Poisson-Boltzmann equation was proposed as the first nonlinear nonlocal dielectric continuum model for computing electrostatics of ionic solvated biomolecules [17]. Meanwhile, to validate our finite element algorithms and program packages for solving these nonlocal models, the analytical solutions of three nonlocal Born ball test models (including the Lorentz nonlocal model) were obtained in [18].

As a continuation of the current studies, in this paper, we first revisit our nonlocal Poisson model and the traditional Lorentz nonlocal model. We then construct two nonlocal Poisson dielectric test models, called models 1 and 2, and obtain their analytical solutions on a dielectric sphere containing multiple point charges. Clearly, with different selections of point charges, we can construct different tests for extensively studying and validating a nonlocal dielectric model and its various numerical solvers.

The techniques that we used to find the analytical solutions of models 1 and 2 are different from the ones used in [13,14,19]. Instead of using associated Legendre polynomials P_n^m to construct a traditional double series, we take advantage of the superposition principle and rotational symmetry to express the analytical solution as a simple infinite series in terms of Legendre polynomials P_n and modified spherical Bessel functions. As a special case of model 1, we also obtain the simple series solution for the classic Poisson dielectric test model. Due to our new simple series expressions, the analytical solutions of models 1 and 2 can be calculated quickly for a large number of point charges on a large set of mesh points, making them valuable and practical in the study of local and nonlocal dielectric models as well as in the validation of related numerical solvers—a critical step before applying the models and solvers to applications.

During the search for an analytical solution, we used convolution techniques to reformulate model 1 or model 2

---
[*]Corresponding author: dxie@uwm.edu

from an integro-differential equation problem into a system of coupled partial differential equations. Thus, it becomes necessary for us to validate the obtained analytical solutions. We proved that our obtained series solutions satisfy the original problems by substituting them to the original integro-differential equations of models 1 and 2. Moreover, we showed that our series solutions converge absolutely with a geometric series rate of convergence. These validation and convergence analyses are difficult and lengthy in writing. They will be reported in another paper since they mainly involve the issues of mathematical analysis.

To simplify the usages and applications, we programed our new series solutions in FORTRAN 90 as an open software source. With this software package, we also can calculate the convolution of solution for model 1 and the reaction parts of the analytical solutions, which can be applied to the development of numerical algorithms for solving local and nonlocal dielectric models [16,17,20]. We further added a special data input option to input the required atomic charge numbers and positions directly from a PQR file of protein, which can be produced from a protein data bank (PDB) file by using the program tool PDB2PQR [21]. Here a PDB file can be downloaded for free from the Protein Data Bank [22]. In this way, we can use different protein molecules to construct different validation tests easily. Finally, we present a test example constructed from a protein to demonstrate the differences between models 1 and 2 and the differences between local and nonlocal models.

The remaining sections of the paper are outlined as follows. In Sec. II, we review the derivation of nonlocal models and define models 1 and 2. In Sec. III, we present the analytical solution of model 1. In Sec. IV, we present the solution of model 2. In Sec. V, we report the program package and test results. In Sec. VI, we make conclusions. Some formulas and series expressions used in this paper are collected in Appendices A and B for clarity.

II. TWO NONLOCAL POISSON DIELECTRIC TEST MODELS

In this section, we review the derivation of local and nonlocal Poisson dielectric models for a protein immersed in water. We then present two nonlocal Poisson test models and a local Poisson test model.

According to Gauss's law, an electrostatic field, **e**, induced by a fixed charge density $\rho(\mathbf{r})$ can be defined by

$$\epsilon_0 \nabla \cdot \mathbf{e}(\mathbf{r}) = \gamma(\mathbf{r}) + \rho(\mathbf{r}) \quad \text{for } \mathbf{r} = (x, y, z) \in \mathbf{R}^3, \quad (1)$$

where ϵ_0 is the permittivity of the vacuum, γ is a dielectric charge density, and $\nabla = (\frac{\partial}{\partial x}, \frac{\partial}{\partial y}, \frac{\partial}{\partial z})$ is the gradient operator. Since **e** is conservative, there exists an electrostatic potential function, Φ, such that

$$\mathbf{e}(\mathbf{r}) = -\nabla \Phi(\mathbf{r}). \quad (2)$$

Applying (2) to (1) yields the Poisson equation:

$$-\Delta \Phi(\mathbf{r}) = \frac{1}{\epsilon_0} [\gamma(\mathbf{r}) + \rho(\mathbf{r})] \quad \forall \mathbf{r} \in \mathbf{R}^3,$$

where $\Phi(\mathbf{r}) \to 0$ as $|\mathbf{r}| \to \infty$, and Δ denotes the Laplace operator. Here $|\mathbf{r}| = \sqrt{x^2 + y^2 + z^2}$ for $\mathbf{r} = (x, y, z)^T$ in the column vector form.

However, it is difficult to estimate γ. To avoid this difficulty, the classic linear dielectric theory (see [23,24], for example) has been developed by assuming that **e** is split into displacement field **d** and polarization field **p**,

$$\epsilon_0 \mathbf{e} = \mathbf{d} - \mathbf{p},$$

where **d** and **p** are defined by

$$(a) \nabla \cdot \mathbf{d}(\mathbf{r}) = \rho(\mathbf{r}), \quad (b) -\nabla \cdot \mathbf{p}(\mathbf{r}) = \gamma(\mathbf{r}), \quad (3)$$

and have the linear relationships with the electric field **e**:

$$(a) \mathbf{d}(\mathbf{r}) = \epsilon_0 \varepsilon(\mathbf{r}) \mathbf{e}(\mathbf{r}), \quad (b) \mathbf{p}(\mathbf{r}) = \epsilon_0 \chi(\mathbf{r}) \mathbf{e}(\mathbf{r}). \quad (4)$$

Here, ε is the dielectric permittivity function, and χ is the susceptibility function. Applying 4(a) and (2) to 3(a), we obtain the local Poisson dielectric model:

$$-\epsilon_0 \nabla \cdot [\varepsilon(\mathbf{r}) \nabla \Phi(\mathbf{r})] = \rho(\mathbf{r}) \quad \forall \mathbf{r} \in \mathbf{R}^3, \quad (5)$$

where $\Phi(\mathbf{r}) \to 0$ as $|\mathbf{r}| \to \infty$.

For a protein immersed in water, $\mathbf{R}^3$ is decomposed by

$$\mathbf{R}^3 = D_p \cup D_s \cup \Gamma,$$

where D_p is the protein region, D_s is the solvent region surrounding D_p, and Γ is an interface between D_p and D_s. According to the continuum implicit solvent theory (see [25], for example), both D_p and D_s can be treated as dielectric continuum media with two different dielectric permittivity constants, ϵ_p and ϵ_s, respectively. In this case, ε becomes a piecewise constant function. To make sense in strong derivatives, the Poisson model (5) should be reformulated into the interface problem:

$$-\epsilon_p \Delta \Phi(\mathbf{r}) = \frac{1}{\epsilon_0} \rho(\mathbf{r}), \quad \mathbf{r} \in D_p, \quad \Delta \Phi(\mathbf{r}) = 0, \quad \mathbf{r} \in D_s,$$

$$\Phi(s^-) = \Phi(s^+), \quad \epsilon_p \frac{\partial \Phi(s^-)}{\partial \mathbf{n}(s)} = \epsilon_s \frac{\partial \Phi(s^+)}{\partial \mathbf{n}(s)}, \quad s \in \Gamma,$$

$$\Phi(\mathbf{r}) \to 0 \quad \text{as } |\mathbf{r}| \to \infty, \quad (6)$$

where $\mathbf{n}(s)$ is the unit outward normal vector of D_p, $\frac{\partial \Phi(s)}{\partial \mathbf{n}(s)} = \nabla \Phi(s) \cdot \mathbf{n}(s)$, $\Phi(s^\pm) = \lim_{t \to 0^+} \Phi[s \pm t\mathbf{n}(s)]$, and $\frac{\partial \Phi(s^\pm)}{\partial \mathbf{n}(s)} = \lim_{t \to 0^+} \frac{\partial \Phi[s \pm t\mathbf{n}(s)]}{\partial \mathbf{n}(s)}$. If a molecular structure of the protein is given, $\rho(\mathbf{r})$ can be estimated by

$$\rho(\mathbf{r}) = e_c \sum_{j=1}^{n_p} z_j \delta(\mathbf{r} - \mathbf{r}_j), \quad (7)$$

where e_c is the elementary charge, n_p is the number of atoms of the protein, $\mathbf{r}_j$ and z_j denote the position and charge number of atom j, respectively, and $\delta(\mathbf{r} - \mathbf{r}_j)$ denotes the Dirac delta distribution at $\mathbf{r}_j$.

It has been known that the relationship (4) can depend on a spatial wave number (see [26], for example). To reflect this feature, the nonlocal dielectric approach was proposed to imitate the linear relationships of (4) in the Fourier frequency space as follows:

$$(a) \quad \widehat{\mathbf{d}}(\xi) = \epsilon_0 \widehat{\varepsilon}(\xi) \widehat{\mathbf{e}}(\xi); \quad (b) \quad \widehat{\mathbf{p}}(\xi) = \epsilon_0 \widehat{\chi}(\xi) \widehat{\mathbf{e}}(\xi), \quad (8)$$

where $\widehat{\varepsilon}(\xi)$, $\widehat{\chi}(\xi)$, $\widehat{\mathbf{d}}(\xi)$, $\widehat{\mathbf{p}}(\xi)$, and $\widehat{\mathbf{e}}(\xi)$ denote the Fourier transforms of $\varepsilon(\mathbf{r})$, $\chi(\mathbf{r})$, $\mathbf{d}(\mathbf{r})$, $\mathbf{p}(\mathbf{r})$, and $\mathbf{e}(\mathbf{r})$, respectively. Applying the inverse Fourier transform to (8) results in the nonlocal relationships of $\mathbf{d}$ and $\mathbf{p}$ with $\mathbf{e}$:

$$\mathbf{d}(\mathbf{r}) = \epsilon_0 \int_{\mathbf{R}^3} \varepsilon(\mathbf{r} - \mathbf{r}')\mathbf{e}(\mathbf{r}')\,d\mathbf{r}', \qquad (9a)$$

$$\mathbf{p}(\mathbf{r}) = \epsilon_0 \int_{\mathbf{R}^3} \chi(\mathbf{r} - \mathbf{r}')\mathbf{e}(\mathbf{r}')\,d\mathbf{r}'. \qquad (9b)$$

Substituting (9a) and (2) to 3(a) yields the nonlocal Poisson equation

$$-\nabla \cdot \int_{\mathbf{R}^3} \varepsilon(\mathbf{r} - \mathbf{r}')\nabla\Phi(\mathbf{r}')\,d\mathbf{r}' = \frac{1}{\epsilon_0}\rho(\mathbf{r}) \quad \forall \mathbf{r} \in \mathbf{R}^3, \quad (10)$$

where $\Phi(\mathbf{r}) \to 0$ as $|\mathbf{r}| \to \infty$.

To reflect the spatial-frequency dependence of a dielectric medium [2,27], a new parameter, λ, for characterizing the polarization correlations of water molecules, and another dielectric constant, ϵ_∞, for water in the case $\lambda \to \infty$, are introduced to result in a commonly used formulation of ε as

$$\varepsilon(\mathbf{r}) = \epsilon_\infty \delta(\mathbf{r}) + (\epsilon_s - \epsilon_\infty)\frac{e^{-|\mathbf{r}|/\lambda}}{4\pi\lambda^2|\mathbf{r}|} \quad \forall \mathbf{r} \in \mathbf{R}^3, \quad (11)$$

where $\epsilon_s > \epsilon_\infty$. Actually, the above permittivity function $\varepsilon(\mathbf{r})$ is the inverse Fourier transform of Debye's temporal frequency dependent permittivity function

$$\widehat{\varepsilon}(\xi) = \epsilon_\infty + \frac{\epsilon_s - \epsilon_\infty}{1 + \lambda^2|\xi|^2}, \qquad (12)$$

where ξ reflects a temporal frequency proportional to a spatial wave number for plane waves (see [[1], p. 100] and [26], for example).

For the protein case, we have shown in our previous work [18] that ε can be modified as a function of two variables $\mathbf{r}$ and $\mathbf{r}'$ in the form

$$\varepsilon(\mathbf{r},\mathbf{r}') = \epsilon(\mathbf{r})\delta(\mathbf{r} - \mathbf{r}') + \kappa(\mathbf{r})Q_\lambda(\mathbf{r} - \mathbf{r}'), \qquad (13)$$

where $\epsilon(\mathbf{r}) = \epsilon_p$ and $\kappa(\mathbf{r}) = 0$ for $\mathbf{r} \in D_p$, $\epsilon(\mathbf{r}) = \epsilon_\infty$ and $\kappa(\mathbf{r}) = \epsilon_s - \epsilon_\infty$ for $\mathbf{r} \in D_s$, and

$$Q_\lambda(\mathbf{r}) = \frac{e^{-|\mathbf{r}|/\lambda}}{4\pi\lambda^2|\mathbf{r}|}. \qquad (14)$$

Applying (13) to (10) gives the nonlocal Poisson model for protein in water with ρ being given in (7):

$$-\epsilon_p \Delta\Phi_p(\mathbf{r}) = \frac{1}{\epsilon_0}\rho(\mathbf{r}), \quad \mathbf{r} \in D_p, \qquad (15a)$$

$$\epsilon_\infty \Delta\Phi_s(\mathbf{r}) + (\epsilon_s - \epsilon_\infty)\nabla \cdot \mathbf{v}(\mathbf{r}) = 0, \quad \mathbf{r} \in D_s, \qquad (15b)$$

$$\Phi_p(\mathbf{s}) = \Phi_s(\mathbf{s}), \quad \mathbf{s} \in \Gamma, \qquad (15c)$$

$$\epsilon_p \frac{\partial\Phi_p(\mathbf{s})}{\partial\mathbf{n}(\mathbf{s})} = \epsilon_\infty \frac{\partial\Phi_s(\mathbf{s})}{\partial\mathbf{n}(\mathbf{s})}$$
$$+ (\epsilon_s - \epsilon_\infty)\mathbf{v}(\mathbf{s}) \cdot \mathbf{n}(\mathbf{s}), \quad \mathbf{s} \in \Gamma, \qquad (15d)$$

where $\Phi_s(\mathbf{r}) \to 0$ as $|\mathbf{r}| \to \infty$, and $\mathbf{v}$ is defined by

$$\mathbf{v}(\mathbf{r}) = \int_{\mathbf{R}^3} Q_\lambda(\mathbf{r} - \mathbf{r}')\nabla\Phi(\mathbf{r}')\,d\mathbf{r}'. \qquad (16)$$

When the integral domain of (16) is changed to D_s (i.e., limited to the consideration of the permittivity correlations among water molecules), the model (15) is modified to another nonlocal Poisson model for protein in water considered in [28, Eq. (4.25), p. 68]. We then construct two test models, called models 1 and 2, for these two nonlocal models using a spherical solute region, $D_p = \{\mathbf{r}:|\mathbf{r}| < a\}$, from which we have $\Gamma = \{\mathbf{r} : |\mathbf{r}| = a\}$ and $D_s = \{\mathbf{r} : |\mathbf{r}| > a\}$. Specially, setting $\epsilon_\infty = \epsilon_s$, we reduce model 1 or model 2 to a local Poisson test model— the Poisson dielectric model (6) using the spherical solute region D_p.

III. ANALYTICAL SOLUTION OF MODEL 1

Let $i_n(r)$ and $k_n(r)$ denote the modified spherical Bessel functions of the first and second kind, respectively, and P_n be a Legendre polynomial of order n. Their definitions and properties can be found in Appendix A. For the charge density ρ given in (7), from the superposition principle we can obtain the analytical solution Φ of model 1 and its convolution $\Phi * Q_\lambda$ in the expressions

$$\Phi(\mathbf{r}) = \frac{e_c}{\epsilon_0} \sum_{j=1}^{n_p} z_j \Phi_j(\mathbf{r}), \quad \mathbf{r} \in \mathbf{R}^3, \qquad (17a)$$

$$(\Phi * Q_\lambda)(\mathbf{r}) = \frac{e_c}{\epsilon_0} \sum_{j=1}^{n_p} z_j (\Phi_j * Q_\lambda)(\mathbf{r}), \quad \mathbf{r} \in \mathbf{R}^3, \qquad (17b)$$

where Φ_j denotes the solution of (15) using $\rho(\mathbf{r}) = \delta(\mathbf{r} - \mathbf{r}_j)$, and Q_λ is given in (14). Thus, the problem is reduced to find each Φ_j and its convolution $\Phi_j * Q_\lambda$.

Theorem 1. Let $\kappa = \frac{1}{\lambda}\sqrt{\frac{\epsilon_s}{\epsilon_\infty}}$. The solution Φ_j of model 1 using $\rho(\mathbf{r}) = \delta(\mathbf{r} - \mathbf{r}_j)$ is given by

$$\Phi_j(\mathbf{r}) = \begin{cases} \sum_{n=0}^\infty A_{3n}|\mathbf{r}|^n P_n\left(\frac{\mathbf{r}_j \cdot \mathbf{r}}{|\mathbf{r}_j||\mathbf{r}|}\right) \\ \quad + \frac{1}{4\pi\epsilon_p|\mathbf{r} - \mathbf{r}_j|}, \quad \mathbf{r} \in D_p, \\ \sum_{n=0}^\infty \left[\frac{\epsilon_\infty - \epsilon_s}{\epsilon_\infty}A_{2n}k_n(\kappa|\mathbf{r}|)\right. \\ \quad \left. + \frac{A_{1n}}{|\mathbf{r}|^{n+1}}\right]P_n\left(\frac{\mathbf{r}_j \cdot \mathbf{r}}{|\mathbf{r}_j||\mathbf{r}|}\right), \quad \mathbf{r} \in D_s, \end{cases} \qquad (18)$$

and its convolution is given by

$$(\Phi_j * Q_\lambda)(\mathbf{r}) = \begin{cases} \frac{1 - e^{-\frac{|\mathbf{r} - \mathbf{r}_j|}{\lambda}}}{4\pi\epsilon_p|\mathbf{r} - \mathbf{r}_j|} + \sum_{n=0}^\infty \left[A_{4n}i_n\left(\frac{|\mathbf{r}|}{\lambda}\right)\right. \\ \quad \left. + A_{3n}|\mathbf{r}|^n\right]P_n\left(\frac{\mathbf{r}_j \cdot \mathbf{r}}{|\mathbf{r}_j||\mathbf{r}|}\right), \quad \mathbf{r} \in D_p, \\ \sum_{n=0}^\infty \left[A_{2n}k_n(\kappa|\mathbf{r}|)\right. \\ \quad \left. + \frac{A_{1n}}{|\mathbf{r}|^{n+1}}\right]P_n\left(\frac{\mathbf{r}_j \cdot \mathbf{r}}{|\mathbf{r}_j||\mathbf{r}|}\right), \quad \mathbf{r} \in D_s, \end{cases} \qquad (19)$$

where A_{in} for $i = 1,2,3,4$ are given by

$$A_{1n} = \frac{2n+1}{4\pi d_n a}\left[\left(\frac{|\mathbf{r}_j|}{a}\right)^n w_n \right.$$
$$\left. + \frac{n\lambda(\epsilon_\infty - \epsilon_s)}{a\epsilon_\infty}i_n\left(\frac{|\mathbf{r}_j|}{\lambda}\right)k_n(\kappa a)\right], \qquad (20a)$$

$$A_{2n} = \frac{(2n+1)\lambda}{4\pi\epsilon_p d_n a^{n+3}}\left[(\epsilon_s - \epsilon_p)(n+1)\frac{|\mathbf{r}_j|^n}{a^n}i_n\left(\frac{a}{\lambda}\right) \right.$$
$$\left. - [n(\epsilon_p + \epsilon_s) + \epsilon_s]i_n\left(\frac{|\mathbf{r}_j|}{\lambda}\right)\right], \qquad (20b)$$

$$A_{3n} = \frac{A_{1n}}{a^{2n+1}} + A_{2n}\frac{\epsilon_\infty - \epsilon_s}{\epsilon_\infty a^n}k_n(\kappa a) - \frac{|\mathbf{r}_j|^n}{4\pi\epsilon_p a^{2n+1}}, \quad (20c)$$

$$A_{4n} = \frac{\frac{2n+1}{2\pi^2\epsilon_p\lambda}i_n\left(\frac{|\mathbf{r}_j|}{\lambda}\right)k_n\left(\frac{a}{\lambda}\right) + A_{2n}\frac{\epsilon_s}{\epsilon_\infty}k_n(\kappa a)}{i_n\left(\frac{a}{\lambda}\right)}. \quad (20d)$$

Here d_n and w_n are defined by

$$d_n = \frac{n(2n+1)\lambda\epsilon_p(\epsilon_s - \epsilon_\infty)}{a^{n+2}\epsilon_\infty}i_n\left(\frac{a}{\lambda}\right)k_n(\kappa a)$$

$$+ \frac{n\epsilon_p + (n+1)\epsilon_s}{a^{n+1}}\left[\frac{\epsilon_s}{\epsilon_\infty}i_{n+1}\left(\frac{a}{\lambda}\right)k_n(\kappa a)\right.$$

$$\left. + \kappa\lambda i_n\left(\frac{a}{\lambda}\right)k_{n+1}(\kappa a)\right], \quad (21)$$

$$w_n = \frac{n\lambda}{a}\frac{\epsilon_s - \epsilon_\infty}{\epsilon_\infty}i_n\left(\frac{a}{\lambda}\right)k_n(\kappa a)$$

$$+ \frac{\epsilon_s}{\epsilon_\infty}i_{n+1}\left(\frac{a}{\lambda}\right)k_n(\kappa a) + \kappa\lambda i_n\left(\frac{a}{\lambda}\right)k_{n+1}(\kappa a). \quad (22)$$

Proof. From the PDE theory (see [29], for example) it is known that $\nabla[\Phi(\mathcal{O}\mathbf{r})] = \mathcal{O}^T(\nabla\Phi)(\mathcal{O}\mathbf{r})$, $\nabla\cdot[\mathbf{F}(\mathcal{O}\mathbf{r})] = [\nabla\cdot(\mathcal{O}\mathbf{F})](\mathcal{O}\mathbf{r})$, and $(\Delta\Phi)(\mathcal{O}\mathbf{r}) = \Delta[\Phi(\mathcal{O}\mathbf{r})]$. Here, $\mathcal{O}$ denotes an orthogonal 3×3 matrix, and $\mathbf{F}$ is a vector function on $\mathbf{R}^3$. Thus, the key step to find Φ_j is to look for the solution Φ of (15) using $\rho(\mathbf{r}) = \delta(\mathbf{r} - \tilde{\mathbf{r}}_j)$ with $\tilde{\mathbf{r}}_j = (0,0,|\mathbf{r}_j|)^T$. We then can obtain Φ_j by

$$\Phi_j(\mathbf{r}) = \Phi(\mathcal{O}_j\mathbf{r}), \quad \mathbf{r} \in \mathbf{R}^3, \quad (23)$$

where $\mathcal{O}_j$ is an orthogonal matrix satisfying $\mathcal{O}_j\mathbf{r}_j = \tilde{\mathbf{r}}_j$.

Since the charge point $\tilde{\mathbf{r}}_j$ lies on the z axis, Φ and its convolution have rotational symmetry about the z axis. That is, they depend only on r and ϕ in the spherical coordinate system (r,θ,ϕ) defined by

$$\mathbf{r} = (r\sin\phi\cos\theta, r\sin\phi\sin\theta, r\cos\phi), \quad (24)$$

where $r > 0$ is the radial distance, $\theta \in [0,2\pi]$ is the azimuthal angle, and $\phi \in [0,\pi]$ is the polar angle.

We set $u = \Phi * Q_\lambda$, $\Phi_p = \Phi$, and $u_p = u$ in D_p, and $\Phi_s = \Phi$ and $u_s = u$ in D_s. As shown in [18], we can reformulate the model (15) as the PDE system

$$-\epsilon_p\Delta\Phi_p(\mathbf{r}) = \delta(\mathbf{r} - \tilde{\mathbf{r}}_j), \quad \mathbf{r} \in D_p, \quad (25a)$$

$$-\lambda^2\Delta u_p(\mathbf{r}) + u_p(\mathbf{r}) - \Phi_p(\mathbf{r}) = 0, \quad \mathbf{r} \in D_p, \quad (25b)$$

$$\epsilon_\infty\Delta\Phi_s + (\epsilon_s - \epsilon_\infty)\Delta u_s = 0, \quad \mathbf{r} \in D_s, \quad (25c)$$

$$-\lambda^2\Delta u_s + u_s - \Phi_s = 0, \quad \mathbf{r} \in D_s, \quad (25d)$$

subject to the interface conditions: For $s\in\Gamma$,

$$u_p(s) = u_s(s), \quad \Phi_p(s) = \Phi_s(s), \quad \frac{\partial u_p(s)}{\partial\mathbf{n}(s)} = \frac{\partial u_s(s)}{\partial\mathbf{n}(s)}, \quad (26a)$$

$$\epsilon_p\frac{\partial\Phi_p(s)}{\partial\mathbf{n}(s)} = \epsilon_\infty\frac{\partial\Phi_s(s)}{\partial\mathbf{n}(s)} + (\epsilon_s - \epsilon_\infty)\frac{\partial u_s(s)}{\partial\mathbf{n}(s)}, \quad (26b)$$

and $\Phi_s(\mathbf{r}) \to 0$ and $u_s(\mathbf{r}) \to 0$ as $|\mathbf{r}| \to \infty$.

From (25c) we obtain

$$\Delta[\epsilon_\infty\Phi_s + (\epsilon_s - \epsilon_\infty)u_s] = 0,$$

implying that $\epsilon_\infty\Phi_s + (\epsilon_s - \epsilon_\infty)u_s$ is harmonic in D_s and converges to 0 as $|\mathbf{r}| \to \infty$.

By Theorem 3 in Appendix B, we get

$$\epsilon_\infty\Phi_s(\mathbf{r}) + (\epsilon_s - \epsilon_\infty)u_s(\mathbf{r}) = \epsilon_s\sum_{n=0}^{\infty}\frac{A_{1n}}{r^{n+1}}P_n(\cos\phi). \quad (27)$$

By (25d) and (27), we get an inhomogeneous linear PDE:

$$-\lambda^2\frac{\epsilon_\infty}{\epsilon_s}\Delta\Phi_s(\mathbf{r}) + \Phi_s(\mathbf{r}) = \sum_{n=0}^{\infty}A_{1n}r^{-n-1}P_n(\cos\phi).$$

The right-hand side is a particular solution, while the general solution of the homogeneous equation is given by Theorem 4 in Appendix B. Hence, we obtain

$$\Phi_s(\mathbf{r}) = \sum_{n=0}^{\infty}\left[\frac{\epsilon_\infty - \epsilon_s}{\epsilon_\infty}A_{2n}k_n(\kappa r) + \frac{A_{1n}}{r^{n+1}}\right]P_n(\cos\phi), \quad (28)$$

where $\phi \in [0,\pi]$. Together with (27), we have

$$u_s(\mathbf{r}) = \sum_{n=0}^{\infty}\left[A_{2n}k_n(\kappa r) + \frac{A_{1n}}{r^{n+1}}\right]P_n(\cos\phi). \quad (29)$$

By Theorem 3, the general solution of (25a) is found as

$$\Phi_p(\mathbf{r}) = \frac{1}{4\pi\epsilon_p}\frac{1}{|\mathbf{r} - \tilde{\mathbf{r}}_j|} + \sum_{n=0}^{\infty}A_{3n}r^n P_n(\cos\phi). \quad (30)$$

A particular solution to the linear inhomogeneous PDE defined by (25b) is given by

$$\frac{1}{4\pi\epsilon_p}\frac{1}{|\mathbf{r} - \tilde{\mathbf{r}}_j|} - \frac{1}{4\pi\epsilon_p}\frac{e^{-|\mathbf{r} - \tilde{\mathbf{r}}_j|/\lambda}}{|\mathbf{r} - \tilde{\mathbf{r}}_j|} + \sum_{n=0}^{\infty}A_{3n}r^n P_n(\cos\phi).$$

Note that the first two terms have a singularity at $\mathbf{r} = \tilde{\mathbf{r}}_j$ but their difference is smooth at $\mathbf{r} = \tilde{\mathbf{r}}_j$. Thus, by Theorem 4, the general solution is given by

$$u_p = \frac{1-e^{-|\mathbf{r}-\tilde{\mathbf{r}}_j|/\lambda}}{4\pi\epsilon_p|\mathbf{r}-\tilde{\mathbf{r}}_j|} + \sum_{n=0}^{\infty}\left[A_{4n}i_n\left(\frac{r}{\lambda}\right) + A_{3n}r^n\right]P_n(\cos\phi). \quad (31)$$

We next determine the coefficients using the interface conditions of the PDE system (25). Together with (B1) and (B2), we can obtain the following system:

$$\frac{A_{1n}}{a^{n+1}} + A_{2n}\frac{\epsilon_\infty - \epsilon_s}{\epsilon_\infty}k_n(\kappa a) - A_{3n}a^n = \frac{|\mathbf{r}_j|^n}{4\pi\epsilon_p a^{n+1}}, \quad (32a)$$

$$A_{1n}\frac{\epsilon_s(n+1)}{\epsilon_p a^{n+2}} + A_{3n}na^{n-1} = \frac{|\mathbf{r}_j|^n(n+1)}{4\pi\epsilon_p a^{n+2}}, \quad (32b)$$

$$\frac{A_{1n}}{a^{n+1}} + A_{2n}k_n(\kappa a) - A_{3n}a^n - A_{4n}i_n\left(\frac{a}{\lambda}\right)$$

$$= \frac{|\mathbf{r}_j|^n}{4\pi\epsilon_p a^{n+1}} - \frac{2n+1}{2\pi^2\epsilon_p\lambda}i_n\left(\frac{|\mathbf{r}_j|}{\lambda}\right)k_n\left(\frac{a}{\lambda}\right), \quad (32c)$$

$$A_{1n}\frac{n+1}{a^{n+2}} - A_{2n}\kappa k_n'(\kappa a) + A_{3n}na^{n-1} + \frac{A_{4n}}{\lambda}i_n'\left(\frac{a}{\lambda}\right)$$

$$= \frac{(n+1)|\mathbf{r}_j|^n}{4\pi\epsilon_p a^{n+2}} + \frac{2n+1}{2\pi^2\epsilon_p\lambda^2}i_n\left(\frac{|\mathbf{r}_j|}{\lambda}\right)k_n'\left(\frac{a}{\lambda}\right). \quad (32d)$$

By subtracting (32a) from (32c), and subtracting (32d) from (32b), we find

$$\frac{\epsilon_s}{\epsilon_\infty} A_{2n} k_n(\kappa a) - A_{4n} i_n\left(\frac{a}{\lambda}\right) = -\frac{2n+1}{2\pi^2 \epsilon_p \lambda} i_n\left(\frac{|\mathbf{r}_j|}{\lambda}\right) k_n\left(\frac{a}{\lambda}\right),$$
(33)

$$A_{1n} \frac{\epsilon_s - \epsilon_p}{\epsilon_p a^{n+2}} (n+1) + A_{2n} \kappa k_n'(\kappa a) - \frac{A_{4n}}{\lambda} i_n'\left(\frac{a}{\lambda}\right)$$

$$= -\frac{2n+1}{2\pi^2 \epsilon_p \lambda^2} i_n\left(\frac{|\mathbf{r}_j|}{\lambda}\right) k_n'\left(\frac{a}{\lambda}\right).$$
(34)

By eliminating A_{3n} from (32a), (32b) and A_{4n} from (33), (34) using the Wronskian (A9), we obtain

$$\begin{pmatrix} \frac{n\epsilon_p + (n+1)\epsilon_s}{a^{n+1}} & n\epsilon_p \frac{\epsilon_\infty - \epsilon_s}{\epsilon_\infty} k_n(\kappa a) \\ \frac{\epsilon_p - \epsilon_s}{\epsilon_p} \frac{n+1}{a^{n+2}} \lambda i_n\left(\frac{a}{\lambda}\right) & w_n \end{pmatrix} \begin{pmatrix} A_{1n} \\ A_{2n} \end{pmatrix}$$

$$= \begin{pmatrix} \frac{|\mathbf{r}_j|^n}{4\pi} \frac{2n+1}{a^{n+1}} \\ -\frac{(2n+1)}{4\pi\epsilon_p a^2} \lambda i_n\left(\frac{|\mathbf{r}_j|}{\lambda}\right) \end{pmatrix},$$
(35)

where $w_n = \frac{\epsilon_s}{\epsilon_\infty} k_n(\kappa a) i_n'\left(\frac{a}{\lambda}\right) - \lambda \kappa k_n'(\kappa a) i_n\left(\frac{a}{\lambda}\right)$, which can be written to (22) by (A4) and (A6).

We determine A_{1n} and A_{2n} from the linear system (35). Using (22), we find its coefficient determinant d_n in the expression (21). Since $i_n(r) > 0$ and $k_n(r) > 0$, and $\epsilon_s \geqslant \epsilon_\infty$, we have $d_n > 0$. Thus, the linear system (35) has the unique solution. Solving it gives A_{1n} and A_{2n}. We then can find A_{3n} using (32a) and A_{4n} using (32c).

We now derive the solution Φ_j and its convolution using (23). In fact, for $\tilde{\mathbf{r}}_j = (0,0,|\mathbf{r}_j|)^T = \mathcal{O}_j \mathbf{r}_j$, it is clear that $|\tilde{\mathbf{r}}| = |\mathbf{r}|$, $|\tilde{\mathbf{r}} - \tilde{\mathbf{r}}_j| = |\mathbf{r} - \mathbf{r}_j|$, and $\langle \tilde{\mathbf{r}}_j, \tilde{\mathbf{r}} \rangle = \langle \mathbf{r}_j, \mathbf{r} \rangle$. Here $\langle \cdot, \cdot \rangle$ denotes the angle between two vectors. Note that $\phi = \langle \tilde{\mathbf{r}}_j, \tilde{\mathbf{r}} \rangle$. Hence, the series expressions of Φ_j and $\Phi_j * Q_\lambda$ can be produced from (28), (29), (30), and (31) by substituting r and $\cos\phi$ to $|\mathbf{r}|$ and $\cos\langle \mathbf{r}_j, \mathbf{r} \rangle$, respectively. Since $\cos\langle \mathbf{r}_j, \mathbf{r} \rangle$ can be calculated by

$$\cos\langle \mathbf{r}_j, \mathbf{r} \rangle = \frac{\mathbf{r}_j \cdot \mathbf{r}}{|\mathbf{r}_j||\mathbf{r}|},$$

we obtain the series expressions (18) and (19) of Φ_j and convolution $\Phi_j * Q_\lambda$. This completes the proof. ∎

Setting $\epsilon_\infty = \epsilon_s$, we can derive the analytical solution of local Poisson test model (6) from the solution of model 1. After simplifications, the solution Φ of the local Poisson test model can be written as

$$\Phi(\mathbf{r}) = \begin{cases} \frac{e_c}{\epsilon_0} \sum_{n=0}^{\infty} \sum_{j=1}^{n_p} z_j A_{j,n} |\mathbf{r}|^n P_n\left(\frac{\mathbf{r}_j \cdot \mathbf{r}}{|\mathbf{r}_j||\mathbf{r}|}\right) \\ \quad + \frac{e_c}{4\pi\epsilon_0 \epsilon_p} \sum_{j=1}^{n_p} \frac{z_j}{|\mathbf{r} - \mathbf{r}_j|}, \quad \mathbf{r} \in D_p, \\ \frac{e_c}{\epsilon_0} \sum_{n=0}^{\infty} \sum_{j=1}^{n_p} \frac{z_j B_{j,n}}{|\mathbf{r}|^{n+1}} P_n\left(\frac{\mathbf{r}_j \cdot \mathbf{r}}{|\mathbf{r}_j||\mathbf{r}|}\right), \quad \mathbf{r} \in D_s, \end{cases}$$
(36)

where $A_{j,n}$ and $B_{j,n}$ are given by

$$A_{j,n} = \frac{(\epsilon_p - \epsilon_s)(n+1)|\mathbf{r}_j|^n}{4\pi\epsilon_p a^{2n+1}[n\epsilon_p + (n+1)\epsilon_s]},$$

$$B_{j,n} = \frac{(2n+1)|\mathbf{r}_j|^n}{4\pi[n\epsilon_p + (n+1)\epsilon_s]}.$$

The convolution of the local Poisson test model solution can also be produced from that of model 1's solution.

Specifically, when $n_p = 1$ and $\mathbf{r}_1$ is the origin $(0,0,0)$, the Poisson test model is often referred to as the Born ball model with a central charge ze_c, whose analytical solution can be implied from (36) directly.

IV. ANALYTICAL SOLUTION OF MODEL 2

In this section, we calculate the series solution of model 2—the equations of (15) with the function $\mathbf{v}$ being replaced by

$$\hat{\mathbf{v}}(\mathbf{r}) = \int_{D_s} Q_\lambda(\mathbf{r} - \mathbf{r}') \nabla \Phi_s(\mathbf{r}') d\mathbf{r}'.$$
(37)

Similar to the case of model 1, the solution Φ of model 2 can be written in (17a) so that we only need to calculate the solution Φ_j of model 2 using $\rho(\mathbf{r}) = \delta(\mathbf{r} - \mathbf{r}_j)$.

Theorem 2. The solution Φ_j of model 2 using $\rho(\mathbf{r}) = \delta(\mathbf{r} - \mathbf{r}_j)$ is given by

$$\Phi_j(\mathbf{r}) = \begin{cases} \sum_{n=0}^{\infty} C_{3n} |\mathbf{r}|^n P_n\left(\frac{\mathbf{r}_j \cdot \mathbf{r}}{|\mathbf{r}_j||\mathbf{r}|}\right) \\ \quad + \frac{1}{4\pi\epsilon_p |\mathbf{r} - \mathbf{r}_j|}, \quad \mathbf{r} \in D_p, \quad (38a) \\ \sum_{n=0}^{\infty} \left[\frac{\epsilon_\infty - \epsilon_s}{\epsilon_\infty} C_{2n} k_n(\kappa|\mathbf{r}|) \\ \quad + \frac{C_{1n}}{|\mathbf{r}|^{n+1}}\right] P_n\left(\frac{\mathbf{r}_j \cdot \mathbf{r}}{|\mathbf{r}_j||\mathbf{r}|}\right), \quad \mathbf{r} \in D_s, \quad (38b) \end{cases}$$

where C_{in} for $i = 1,2,3$ are defined by

$$C_{1n} = \frac{2n+1}{4\pi e_n} |\mathbf{r}_j|^n w_n,$$
(39a)

$$C_{2n} = -\frac{(2n+1)(n+1)}{4\pi a^{n+2} e_n} \lambda |\mathbf{r}_j|^n i_n\left(\frac{a}{\lambda}\right),$$
(39b)

$$C_{3n} = \frac{|\mathbf{r}_j|^n}{4\pi a^{2n+1}} \left[\frac{(2n+1)s_n}{e_n} - \frac{1}{\epsilon_p}\right].$$
(39c)

Here e_n, s_n, and w_n are given in (58), (59), and (60), respectively.

Proof. By the same arguments used in the case of model 1, it is sufficient for us to find the solution of model 2 using $\rho(\mathbf{r}) = \delta(\mathbf{r} - \mathbf{r}_0)$ with $\mathbf{r}_0 = (0,0,z_0)$ for $0 < z_0 < a$ in the spherical coordinate system (r,θ,ϕ) defined by (24). In order to simplify calculation, we extend Φ_s continuously to a harmonic function in D_p by

$$\Phi_s(\mathbf{r}) = \sum_{n=0}^{\infty} C_{0n} \left(\frac{r}{a}\right)^n P_n(\cos\phi), \quad \mathbf{r} \in D_p$$
(40)

when Φ_s has the expression on the interface Γ:

$$\Phi_s(\mathbf{s}) = \sum_{n=0}^{\infty} C_{0n} P_n(\cos\phi), \quad \mathbf{s} \in \Gamma,$$
(41)

where C_{0n} are constants to be determined.

To get the analytical solution, we define w by

$$w(\mathbf{r}) = (Q_\lambda * \Phi_s)(\mathbf{r}), \quad \mathbf{r} \in \mathbf{R}^3,$$

and reformulate the function $\hat{\mathbf{v}}$ of (37) as

$$\hat{\mathbf{v}}(\mathbf{r}) = \int_{\mathbf{R}^3} Q_\lambda(\mathbf{r} - \mathbf{r}') \nabla'_{\mathbf{r}} \Phi_s(\mathbf{r}') d\mathbf{r}' - \hat{\mathbf{v}}_0(\mathbf{r}),$$
(42)

where $\hat{\mathbf{v}}_0(\mathbf{r}) = \int_{D_p} Q_\lambda(\mathbf{r} - \mathbf{r}') \nabla_{\mathbf{r}'} \Phi_s(\mathbf{r}') d\mathbf{r}'$.

It is easy to see that w satisfies the equation

$$-\lambda^2 \Delta w(\mathbf{r}) + w(\mathbf{r}) = \Phi_s(\mathbf{r}), \quad \mathbf{r} \in \mathbf{R}^3.$$

Let $h(\mathbf{r}) = \nabla \cdot \hat{\mathbf{v}}_0(\mathbf{r})$. It can be shown [see (B4)] that

$$h(\mathbf{r}) = -\sum_{n=0}^{\infty} C_{0n} \frac{2na}{\pi \lambda^3} i_n\left(\frac{a}{\lambda}\right) k_n\left(\frac{r}{\lambda}\right) P_n(\cos\phi) \quad (43)$$

for $\mathbf{r} \in D_s$. Moreover, for s$\in\Gamma$, by (B5),

$$\hat{\mathbf{v}}_0(s) \cdot \mathbf{n}(s) = \sum_{n=0}^{\infty} C_{0n} \frac{2na}{\pi \lambda^2} i_n\left(\frac{a}{\lambda}\right) k_{n-1}\left(\frac{a}{\lambda}\right) P_n(\cos\phi). \quad (44)$$

We now reformulate Eq. (15) (with $\mathbf{v}$ replaced by $\hat{\mathbf{v}}$) as the following PDE system:

$$-\epsilon_p \Delta \Phi_p(\mathbf{r}) = \delta(\mathbf{r} - \mathbf{r}_0), \quad \mathbf{r} \in D_p, \quad (45a)$$

$$-\lambda^2 \Delta w_p(\mathbf{r}) + w_p(\mathbf{r}) - \Phi_s(\mathbf{r}) = 0, \quad \mathbf{r} \in D_p, \quad (45b)$$

$$\epsilon_\infty \Delta \Phi_s + (\epsilon_s - \epsilon_\infty)[\Delta w_s - h] = 0, \quad \mathbf{r} \in D_s, \quad (45c)$$

$$-\lambda^2 \Delta w_s + w_s - \Phi_s = 0, \quad \mathbf{r} \in D_s, \quad (45d)$$

subject to the interface conditions: For s$\in\Gamma$,

$$w_p(s) = w_s(s), \quad \frac{\partial w_p(s)}{\partial \mathbf{n}(s)} = \frac{\partial w_s(s)}{\partial \mathbf{n}(s)}, \quad (46)$$

$$\Phi_p(s) = \Phi_s(s), \quad \epsilon_p \frac{\partial \Phi_p(s)}{\partial \mathbf{n}(s)} = \epsilon_\infty \frac{\partial \Phi_s(s)}{\partial \mathbf{n}(s)}$$

$$+ (\epsilon_s - \epsilon_\infty)\left[\frac{\partial w_s(s)}{\partial \mathbf{n}(s)} - \hat{\mathbf{v}}_0(s) \cdot \mathbf{n}(s)\right], \quad (47)$$

and $\Phi_s(\mathbf{r}) \to 0$, $w_s(\mathbf{r}) \to 0$ as $|\mathbf{r}| \to \infty$.

We note that h satisfies $\lambda^2 \Delta h = h$ in D_s. Thus, (45c) can be written as

$$\Delta[\epsilon_\infty \Phi_s + (\epsilon_s - \epsilon_\infty)w_s - \lambda^2(\epsilon_s - \epsilon_\infty)h] = 0.$$

By Theorem 3, there are constants C_{1n} such that

$$\epsilon_\infty \Phi_s(\mathbf{r}) + (\epsilon_s - \epsilon_\infty)[w_s(\mathbf{r}) - \lambda^2 h(\mathbf{r})]$$

$$= \epsilon_s \sum_{n=0}^{\infty} C_{1n} r^{-n-1} P_n(\cos\phi) \text{ for } \mathbf{r} \in D_s. \quad (48)$$

From (45c) and (45d) we obtain

$$\epsilon_\infty \Phi_s + (\epsilon_s - \epsilon_\infty)(w_s - \lambda^2 h) = -\lambda^2 \epsilon_\infty \Delta \Phi_s + \epsilon_s \Phi_s.$$

Therefore, using (48), we get

$$-\lambda^2 \frac{\epsilon_\infty}{\epsilon_s} \Delta \Phi_s(\mathbf{r}) + \Phi_s(\mathbf{r}) = \sum_{n=0}^{\infty} \frac{C_{1n}}{r^{n+1}} P_n(\cos\phi),$$

and the right-hand side is a particular solution. Therefore, we obtain (38b) for $\mathbf{r} \in D_s$. From (45a) and (45b), we can obtain (38a).

With (48) and (38b), we get

$$w_s(\mathbf{r}) = \sum_{n=0}^{\infty} C_{1n} r^{-n-1} P_n(\cos\phi)$$

$$+ \sum_{n=0}^{\infty} C_{2n} k_n(\kappa r) P_n(\cos\phi) + \lambda^2 h(\mathbf{r}). \quad (49)$$

For $\mathbf{r} \in D_p$, from (45a) we find

$$\Phi_p(\mathbf{r}) = \frac{1}{4\pi \epsilon_p} \frac{1}{|\mathbf{r} - \mathbf{r}_0|} + \sum_{n=0}^{\infty} C_{3n} r^n P_n(\cos\phi). \quad (50)$$

Then, (45b) gives

$$w_p(\mathbf{r}) = \Phi_s(\mathbf{r}) + \sum_{n=0}^{\infty} C_{4n} i_n\left(\frac{r}{\lambda}\right) P_n(\cos\phi), \quad (51)$$

where $\Phi_s(\mathbf{r})$ is given in (40).

Next, we establish the expressions of coefficients C_{in} for $i = 0$–4. By comparing (41) and (38b), we obtain

$$C_{0n} = \frac{C_{1n}}{a^{n+1}} + \frac{\epsilon_\infty - \epsilon_s}{\epsilon_\infty} C_{2n} k_n(\kappa a). \quad (52)$$

The first interface condition of (47) gives

$$\frac{z_0^n}{4\pi \epsilon_p a^{n+1}} + C_{3n} a^n = C_{0n}. \quad (53)$$

Together with (43) and (44), the second interface condition of (47) gives

$$-(n + 1)\frac{z_0^n}{4\pi a^{n+2}} + \epsilon_p C_{3n} na^{n-1} = -\epsilon_s C_{1n} \frac{n + 1}{a^{n+2}}$$

$$+ (\epsilon_s - \epsilon_\infty) C_{0n} \frac{2n(n + 1)}{\pi \lambda} i_n\left(\frac{a}{\lambda}\right) k_n\left(\frac{a}{\lambda}\right). \quad (54)$$

From the interface conditions of (46), we obtain

$$C_{0n} + C_{4n} i_n\left(\frac{a}{\lambda}\right) = \frac{C_{1n}}{a^{n+1}} + C_{2n} k_n(\kappa a)$$

$$- C_{0n} \frac{2na}{\pi \lambda} i_n\left(\frac{a}{\lambda}\right) k_n\left(\frac{a}{\lambda}\right), \quad (55)$$

and

$$C_{0n} \frac{n}{a} + C_{4n} \frac{1}{\lambda} i_n'\left(\frac{a}{\lambda}\right) = -\frac{C_{1n}(n + 1)}{a^{n+2}} + C_{2n} \kappa k_n'(\kappa a)$$

$$- C_{0n} \frac{2na}{\pi \lambda^2} i_n\left(\frac{a}{\lambda}\right) k_n'\left(\frac{a}{\lambda}\right). \quad (56)$$

By using (52) and eliminating C_{3n} from (53), (54), and C_{4n} from (55), (56), we obtain the linear system

$$\begin{pmatrix} -1 & 1 & \frac{\epsilon_\infty - \epsilon_s}{\epsilon_\infty} k_n(\kappa a) \\ u_n & -\epsilon_s(n + 1) & 0 \\ -i_n'\left(\frac{a}{\lambda}\right) & i_{n-1}\left(\frac{a}{\lambda}\right) & v_n \end{pmatrix} \begin{pmatrix} C_{0n} \\ \tilde{C}_{1n} \\ C_{2n} \end{pmatrix}$$

$$= \begin{pmatrix} 0 \\ -(2n + 1)\frac{z_0^n}{4\pi a^{n+1}} \\ 0 \end{pmatrix}, \quad (57)$$

where $u_n = -n\epsilon_p + (\epsilon_s - \epsilon_\infty)n(n + 1)\frac{2a}{\pi \lambda} i_n\left(\frac{a}{\lambda}\right) k_n\left(\frac{a}{\lambda}\right)$, $\tilde{C}_{1n} = C_{1n}/a^{n+1}$, and

$$v_n = i_{n+1}\left(\frac{a}{\lambda}\right) k_n(\kappa a) + \kappa \lambda i_n\left(\frac{a}{\lambda}\right) k_{n+1}(\kappa a).$$

Then the determinant e_n of the coefficient matrix in (57) is given by

$$e_n = \epsilon_s(n + 1)w_n - u_n s_n, \quad (58)$$

where s_n and w_n can be found as follows:

$$s_n = \begin{vmatrix} 1 & \frac{\epsilon_\infty - \epsilon_s}{\epsilon_\infty} k_n(\kappa a) \\ i_{n-1}\left(\frac{a}{\lambda}\right) & v_n \end{vmatrix}$$

$$= \frac{\epsilon_s - \epsilon_\infty}{\epsilon_\infty} \frac{(2n+1)\lambda}{a} i_n\left(\frac{a}{\lambda}\right) k_n(\kappa a)$$

$$+ \frac{\epsilon_s}{\epsilon_\infty} i_{n+1}\left(\frac{a}{\lambda}\right) k_n(\kappa a) + \kappa \lambda i_n\left(\frac{a}{\lambda}\right) k_{n+1}(\kappa a), \quad (59)$$

$$w_n = \begin{vmatrix} 1 & \frac{\epsilon_\infty - \epsilon_s}{\epsilon_\infty} k_n(\kappa a) \\ i'_n\left(\frac{a}{\lambda}\right) & v_n \end{vmatrix}$$

$$= \frac{\epsilon_s - \epsilon_\infty}{\epsilon_\infty} \frac{n\lambda}{a} i_n\left(\frac{a}{\lambda}\right) k_n(\kappa a)$$

$$+ \frac{\epsilon_s}{\epsilon_\infty} i_{n+1}\left(\frac{a}{\lambda}\right) k_n(\kappa a) + \kappa \lambda i_n\left(\frac{a}{\lambda}\right) k_{n+1}(\kappa a). \quad (60)$$

It follows from (A7) and (A8) that

$$\frac{2n+1}{r} i_n(r) k_n(r) = \frac{\pi}{2r^2} - i_n(r) k_{n-1}(r)$$
$$- i_{n+1}(r) k_n(r) < \frac{\pi}{2r^2}.$$

Therefore, we have

$$u_n \leqslant \epsilon_s n(n+1) \frac{2a}{\pi \lambda} i_n\left(\frac{a}{\lambda}\right) k_n\left(\frac{a}{\lambda}\right) \leqslant \epsilon_s \frac{n(n+1)}{2n+1}.$$

Since $\epsilon_s \geqslant e_\infty$, we have $s_n > 0$ and the estimate

$$e_n \geqslant \epsilon_s \frac{(n+1)^2}{2n+1} \left[\frac{\epsilon_s}{\epsilon_\infty} i_{n+1}\left(\frac{a}{\lambda}\right) k_n(\kappa a) \right.$$
$$\left. + \kappa \lambda i_n\left(\frac{a}{\lambda}\right) k_{n+1}(\kappa a) \right] > 0.$$

Based on the above derivations, we can obtain the solution of the system (57) so that the expressions of C_{in} for $i = 0,1,2$ are found as follows:

$$C_{0n} = (2n+1) \frac{z_0^n}{4\pi a^{n+1}} \frac{s_n}{e_n}, \quad C_{1n} = (2n+1) \frac{z_0^n}{4\pi} \frac{w_n}{e_n},$$

$$C_{2n} = -(2n+1)(n+1) \frac{z_0^n \lambda}{4\pi a^{n+2}} \frac{i_n\left(\frac{a}{\lambda}\right)}{e_n}.$$

Then we obtain C_{3n} and C_{4n} from (52), (53), and (55):

$$C_{3n} = \frac{C_{0n}}{a^n} - \frac{z_0^n}{4\pi \epsilon_p a^{2n+1}}, \quad (61)$$

$$C_{4n} = \frac{C_{2n} \frac{\epsilon_s}{\epsilon_\infty} k_n(\kappa a) - C_{0n} \frac{2na}{\pi \lambda} i_n\left(\frac{a}{\lambda}\right) k_n\left(\frac{a}{\lambda}\right)}{i_n\left(\frac{a}{\lambda}\right)} \quad (62)$$

from which we can get the expressions of (39). This completes the proof. ∎

V. PROGRAM PACKAGE AND TEST RESULTS

We programed the series solutions of models 1 and 2 in FORTRAN 90, along with the series solution of the local Poisson dielectric model (6). We also included the calculation of reaction function Ψ as a part of our FORTRAN program

package. Here, Ψ is defined by

$$\Psi = \Phi - G \quad \text{with} \quad G(\mathbf{r}) = \frac{e_c}{4\pi \epsilon_0 \epsilon_p} \sum_{j=1}^{n_p} \frac{z_j}{|\mathbf{r} - \mathbf{r}_j|}, \quad (63)$$

and both Φ and Ψ are calculated approximately in a partial sum of N terms for a set of given mesh points and a set of point charges. The program package can be downloaded for free from Supplemental Material [30].

To simplify the application of our program package, a PQR file input option is provided to input the charge numbers $\{z_j\}_{j=1}^{n_p}$ and positions $\{\mathbf{r}_j\}_{j=1}^{n_p}$ automatically from a PQR file of a protein. In this case, the center of a protein molecular structure is moved to the origin, and the atomic positions are rescaled to satisfy the condition $|\mathbf{r}_j| < a$. In this way, we can easily construct different tests using different protein molecules. In fact, a PQR file is widely used in the numerical solution of a local or nonlocal dielectric model. It can be produced from a PDB file by using the program tool PDB2PQR [21]. A PDB file can be downloaded for free from the Protein Data Bank [22].

As shown in our previous work [16,20], Ψ can be twice continuously differentiable within and outside D_p and continuous across the interface Γ for local and nonlocal Poisson models. Thus, G contains all the singularity points of Φ. Hence, the singularity difficulty of computing Φ can be completely avoided through computing Ψ.

With our program package (see Supplemental Material [30]), we now can easily construct a test case to demonstrate the importance of developing solution decomposition algorithms for solving local and nonlocal dielectric models. As an example, we considered one set of 488 point charges coming from a protein with 488 atoms (PDB ID: 2LXZ) as illustrated in Fig. 1. Here, we calculated the values of Φ and Ψ at the mesh points of three uniform meshes of a cubic domain $[-2,2]^3$ with mesh size $h = 0.1, 0.05,$ and 0.01 for models 1 and 2 and the local Poisson model using $\epsilon_p = 2, \epsilon_s = 80,$ $\epsilon_\infty = 1.8, \lambda = 10, a = 1,$ and $N = 20$, which was found to
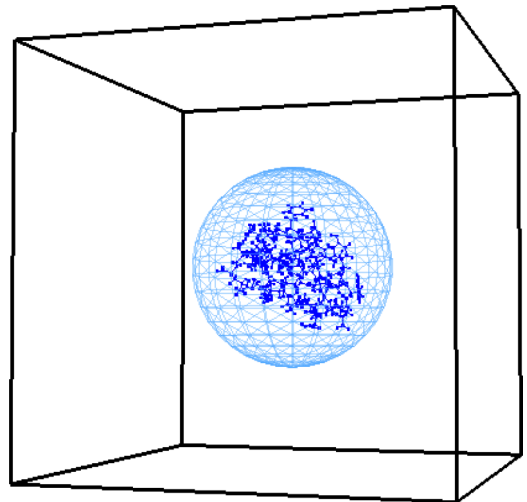

FIG. 1. A unit spherical solute region D_p containing 488 point charges from a protein (2LZX) in a cubic domain $[-2,2]^3$.

yield a solution with a relative error $O(10^{-5})$. The three meshes had 68 921, 531 441, and 4 173 281 mesh points, respectively. Our FORTRAN program package was found very efficient in these calculations. For example, it took only about 13 s in the calculation of 68 921 function values for model 1 on one 3.7 GHz Intel Xeon processor of our Mac Pro workstation.

We also did tests on the simple series solution of the local Poisson test model (6), which is given in (36). The test with 68 921 mesh points, 488 charges, and a partial sum of 20 terms (i.e., $n = 19$) took 12 s while the relative error was found to be 1.99×10^{-5}. As a comparison, we programed the double series solution obtained from the well known Kirkwood's dielectric sphere model [19]. Since the partial sum of this double series consists of $(n + 1)^2$ terms, and each term involves complex numbers, its calculation can be very costly. For the same test as done above, the total CPU time was sharply raised to 1021 s while the relative error was 3.2×10^{-2} only. This test indicated that Kirkwood's dielectric sphere model was ineffective for validation tests.

Using the calculated values of Φ and Ψ, we constructed the linear interpolation functions of Φ and Ψ based on the uniform meshes. We then plotted them by setting $y = 0$ to display one cross section of them in surface graphs on MATLAB as shown in Figs. 2 and 3. Note that each MATLAB surface plot is essentially a linear interpolation of a function on a uniform mesh. Hence, these MATLAB surface plots reflect the convergent behaviors of these interpolation functions.

Figure 2 displays a comparison of model 1 with model 2 and the local Poisson model in terms of reaction function Ψ. From these graphs we can see that models 1 and 2 are very similar while both of them are significantly different from the local model. They all have continuous surfaces. Moreover, their function surfaces are smooth in the solute region D_p and the solvent region D_s, respectively, confirming what was claimed in [16,20].

Figure 3 shows that the linear interpolation functions of Φ became more and more spiky as h was reduced from 0.1 to 0.01, due to the solution singularity caused by the Dirac-delta distributions. Because of so many strongly singular points, it seems impossible for us to numerically solve a dielectric model for Φ directly on a mesh with a small grid size h. To achieve a high accuracy, we have to develop solution decomposition algorithms for computing Φ indirectly through searching for reaction function Ψ.

VI. CONCLUSIONS

In this paper, we have presented two nonlocal dielectric test models, called models 1 and 2, for a spherical solute region containing multiple point charges. We then obtained their analytical solutions in simple series, and validated them analytically. Furthermore, we programed these analytical solutions in FORTRAN as a software package, along with their convolution functions and their reaction parts. The usage of this software package is simple since a set of point charges can be directly input from a PDB file of a protein. Numerical tests demonstrated the high performance of our program package in comparison to the traditional double series approach as done by Kirkwood for a local dielectric sphere model. This
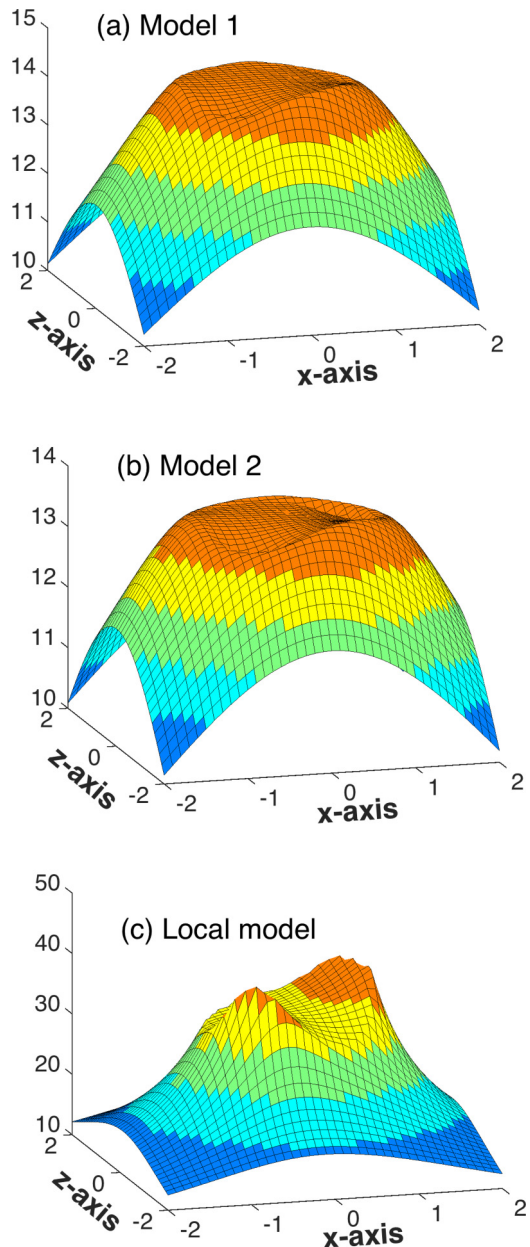

FIG. 2. A comparison of model 1 with model 2 and the local Poisson model in their reaction functions of Ψ defined on a uniform mesh of $[-2,2]^3$ with $h = 0.1$ for the unit spherical solute region D_p containing 488 point charges from a protein (2LXZ).

work is expected to be of wide interest to computational biophysicists and biochemists, applied mathematicians, and bioengineers. The package will be a valuable tool for them to study local and nonlocal models and related numerical solvers.

As applications, numerical test results were used to illustrate that reducing the mesh size may increase the difficulty of solving a dielectric model. Hence, the solution decomposition approach is essential in the development of numerical algorithms for solving a dielectric continuum model efficiently and effectively.
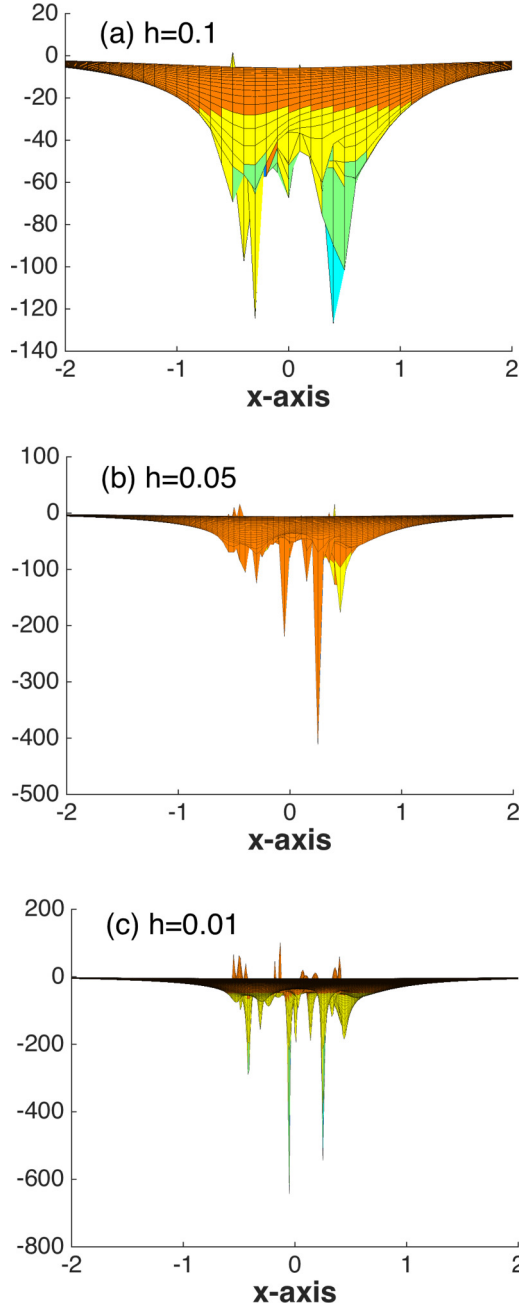
FIG. 3. A comparison of three linear interpolation functions of the analytical solution Φ for model 1 defined on three uniform meshes of $[-2,2]^3$ with $h = 0.1, 0.05,$ and 0.01. Here, D_P contains 488 point charges, and the figures are plotted by setting y coordinates to be zero.

ACKNOWLEDGMENTS

APPENDIX A: MODIFIED SPHERICAL BESSEL FUNCTIONS

We collect some formulas for modified spherical Bessel functions $i_n(r)$ and $k_n(r)$. If not stated otherwise, these formulas can be found in [[31], Sec. 10.47ff.].

We define i_n and k_n in terms of modified Bessel functions I_ν and K_ν by

$$i_n(r) = \sqrt{\frac{\pi}{2r}} I_{n+1/2}(r) = r^n \left(\frac{1}{r}\frac{d}{dr}\right)^n \left(\frac{\sinh r}{r}\right), \quad \text{(A1)}$$

$$k_n(r) = \sqrt{\frac{\pi}{2r}} K_{n+1/2}(r) = (-1)^n \frac{\pi}{2} r^n \left(\frac{1}{r}\frac{d}{dr}\right)^n \left(\frac{e^{-r}}{r}\right). \quad \text{(A2)}$$

Let y' denote the first derivative of function y. We have the formulas:

$$i_n'(r) = -\frac{n+1}{r}i_n(r) + i_{n-1}(r), \quad \text{(A3)}$$

$$i_n'(r) = \frac{n}{r}i_n(r) + i_{n+1}(r), \quad \text{(A4)}$$

$$k_n'(r) = -\frac{n+1}{r}k_n(r) - k_{n-1}(r), \quad \text{(A5)}$$

$$k_n'(r) = \frac{n}{r}k_n(r) - k_{n+1}(r), \quad \text{(A6)}$$

$$i_{n-1}(r) - i_{n+1}(r) = \frac{2n+1}{r}i_n(r), \quad \text{(A7)}$$

$$k_n(r)i_{n+1}(r) + k_{n+1}(r)i_n(r) = \frac{\pi}{2r^2}. \quad \text{(A8)}$$

The Wronskian of i_n and k_n is

$$i_n(r)k_n'(r) - i_n'(r)k_n(r) = -\frac{\pi}{2r^2}. \quad \text{(A9)}$$

APPENDIX B: SERIES EXPRESSIONS OF SOME FUNCTIONS AND SOLUTIONS

Let P_n denote the Legendre polynomial of degree n, (r,θ,ϕ) denote the spherical coordinates, and $\mathbf{r}_0 = (0,0,z_0)$. Here $r = |\mathbf{r}|$. The functions $\frac{1}{|\mathbf{r}-\mathbf{r}_0|}$ and $\frac{e^{-|\mathbf{r}-\mathbf{r}_0|/\lambda}}{|\mathbf{r}-\mathbf{r}_0|}$ can be expanded to the following series expressions [[31], 10.60.3]:

$$\frac{1}{|\mathbf{r}-\mathbf{r}_0|} = \begin{cases} \frac{1}{r}\sum_{n=0}^{\infty}\left(\frac{z_0}{r}\right)^n P_n(\cos\phi) & \text{if } r > z_0, \\ \frac{1}{z_0}\sum_{n=0}^{\infty}\left(\frac{r}{z_0}\right)^n P_n(\cos\phi) & \text{if } r < z_0 \end{cases} \quad \text{(B1)}$$

and

$$\frac{e^{-\frac{|\mathbf{r}-\mathbf{r}_0|}{\lambda}}}{|\mathbf{r}-\mathbf{r}_0|}$$

$$= \frac{2}{\pi\lambda} \begin{cases} \sum_{n=0}^{\infty}(2n+1)i_n(\frac{z_0}{\lambda})k_n(\frac{r}{\lambda})P_n(\cos\phi) & \text{if } r > z_0, \\ \sum_{n=0}^{\infty}(2n+1)i_n(\frac{r}{\lambda})k_n(\frac{z_0}{\lambda})P_n(\cos\phi) & \text{if } r < z_0. \end{cases} \quad \text{(B2)}$$

The following results are known (see [[32], Sec. 5.53], for example).

Theorem 3. If u is a rotationally symmetric solution to the Laplace equation $\Delta u = 0$ in D_p, then there are constants C_n such that

$$u(\mathbf{r}) = \sum_{n=0}^{\infty} C_n r^n P_n(\cos\phi).$$

If u is a rotationally symmetric solution to the Laplace equation $\Delta u = 0$ in D_s with $u(\mathbf{r}) \to 0$ as $|\mathbf{r}| \to \infty$, then there are constants C_n such that

$$u(\mathbf{r}) = \sum_{n=0}^{\infty} C_n r^{-n-1} P_n(\cos\phi).$$

Theorem 4. If u is a rotationally symmetric solution to $\Delta u - \kappa^2 u = 0$, $\kappa > 0$, in D_p, then there are constants C_n such that

$$u(\mathbf{r}) = \sum_{n=0}^{\infty} C_n i_n(\kappa r) P_n(\cos\phi).$$

If u is a rotationally symmetric solution to $\Delta u - \kappa^2 u = 0$, $\kappa > 0$, in D_s with $u(\mathbf{r}) \to 0$ as $|\mathbf{r}| \to \infty$, then there are constants C_n such that

$$u(\mathbf{r}) = \sum_{n=0}^{\infty} C_n k_n(\kappa r) P_n(\cos\phi).$$

Let (r,ϕ,θ) and (r',ϕ',θ') be the spherical coordinates for $\mathbf{r}$ and $\mathbf{r}'$, respectively, and P_n^m be the associated Legendre function, which is defined by

$$P_n^m(t) = (-1)^m (1 - t^2)^{m/2} \frac{d^m}{dt^m} P_n(t)$$

for $m = 0, 1, \ldots, n$. Here $r = |\mathbf{r}|$ and $r' = |\mathbf{r}'|$. We set $D_p = \{\mathbf{r}' \mid |\mathbf{r}'| < a\}$ and $\Gamma = \{\mathbf{r}' \mid |\mathbf{r}'| = a\}$. Then,

$$\int_{\Gamma} Q_\lambda(\mathbf{r} - \mathbf{r}') P_n^m(\cos\phi') \cos(m\theta') dS(\mathbf{r}')$$

$$= \frac{2a^2}{\pi\lambda^3} P_n^m(\cos\phi) \cos(m\theta) \begin{cases} i_n\left(\frac{r}{\lambda}\right) k_n\left(\frac{a}{\lambda}\right) & \text{if } r \leqslant a, \\ i_n\left(\frac{a}{\lambda}\right) k_n\left(\frac{r}{\lambda}\right) & \text{if } r > a. \end{cases} \quad \text{(B3)}$$

This follows from (B2), the addition theorem for Legendre functions and orthogonality of spherical harmonics. A similar formula holds for $P_n^m(\cos\phi) \sin(m\theta)$.

Set $\mathbf{v}(\mathbf{r}) = \int_{D_p} Q_\lambda(\mathbf{r} - \mathbf{r}') \nabla_{\mathbf{r}'}[(r')^n P_n(\cos\phi')] d\mathbf{r}'$. Then

$$(\nabla \cdot \mathbf{v})(\mathbf{r}) = -\int_{D_p} \nabla_{\mathbf{r}'} Q_\lambda(\mathbf{r} - \mathbf{r}') \cdot \nabla_{\mathbf{r}'}[|\mathbf{r}'|^n P_n(\cos\phi') d\mathbf{r}'.$$

By Green's formula and noting that $|\mathbf{r}'|^n P_n(\cos\phi')$ is a harmonic function

$$(\nabla \cdot \mathbf{v})(\mathbf{r}) = -\int_{\Gamma} Q_\lambda(\mathbf{r} - \mathbf{r}') n |\mathbf{r}'|^{n-1} P_n(\cos\phi') dS(\mathbf{r}').$$

Using (B3), we obtain for $r > a$,

$$(\nabla \cdot \mathbf{v})(\mathbf{r}) = -\frac{2na^{n+1}}{\pi\lambda^3} i_n\left(\frac{a}{\lambda}\right) k_n\left(\frac{r}{\lambda}\right) P_n(\cos\phi). \quad \text{(B4)}$$

From [[33], p. 137ff] it is known that

$$\nabla'_{\mathbf{r}}(|\mathbf{r}'|^n P_n \cos\phi')] = |\mathbf{r}'|^{n-1}\langle P_{n-1}^1(\cos\phi)\cos\theta', P_{n-1}^1(\cos\phi)$$
$$\times \sin\theta', n P_{n-1}(\cos\phi')\rangle.$$

Applying (B3) for $r \geqslant a$ gives

$$\mathbf{v}(\mathbf{r}) = \frac{2}{\pi\lambda^3} k_{n-1}\left(\frac{r}{\lambda}\right) \int_0^a (r')^{n+1} i_{n-1}\left(\frac{r'}{\lambda}\right) dr'$$
$$\times \langle P_{n-1}^1(\cos\phi)\cos\theta, P_{n-1}^1(\cos\phi)\sin\theta, n P_{n-1}(\cos\phi)\rangle.$$

Evaluating the above integral by using (A3) gives

$$\mathbf{v}(\mathbf{r}) = \frac{2a^{n+1}}{\pi\lambda^2} i_n\left(\frac{a}{\lambda}\right) k_{n-1}\left(\frac{r}{\lambda}\right)$$
$$\times \langle P_{n-1}^1(\cos\phi)\cos\theta, P_{n-1}^1(\cos\phi)\sin\theta, n P_{n-1}(\cos\phi)\rangle.$$

Let $\mathbf{n}(\mathbf{r})$ be the unit normal. From [[33], p. 33, (31)] it is known that $n\cos\phi P_{n-1}(\cos\phi) + \sin\phi P_{n-1}^1(\cos\phi) = n P_n(\cos\phi)$. Then we obtain on the sphere $|\mathbf{r}| = a$ that

$$\mathbf{v}(\mathbf{r}) \cdot \mathbf{n}(\mathbf{r}) = \frac{2na^{n+1}}{\pi\lambda^2} i_n\left(\frac{a}{\lambda}\right) k_{n-1}\left(\frac{a}{\lambda}\right) P_n(\cos\phi). \quad \text{(B5)}$$

[1] M. V. Basilevsky and G. N. Chuev, in *Continuum Solvation Models in Chemical Physics: From Theory to Applications*, edited by B. Mennucci and R. Cammi (Wiley, New York, 2008), p. 94.

[2] *The Chemical Physics of Solvation. Part A: Theory of Solvation*, edited by R. R. Dogonadze, E. Kálmán, A. A. Kornyshev, and J. Ulstrup, Studies in Physical and Theoretical Chemistry Vol. 38 (Elsevier Science Ltd., Amsterdam, 1985).

[3] A. A. Kornyshev and G. Sutmann, Phys. Rev. Lett. **79**, 3435 (1997).

[4] J. Dai, I. Tsukerman, A. Rubinstein, and S. Sherman, IEEE Trans. Magn. **43**, 1217 (2007).

[5] A. Rubinstein, R. F. Sabirianov, W. N. Mei, F. Namavar, and A. Khoynezhad, Phys. Rev. E **82**, 021915 (2010).

[6] P. A. Bopp, A. A. Kornyshev, and G. Sutmann, Phys. Rev. Lett. **76**, 1280 (1996).

[7] B. Sahin and B. Ralf, J. Phys.: Condens. Matter **26**, 285101 (2014).

[8] L. R. Scott, M. Boland, K. Rogale, and A. Fernández, J. Phys. A: Math. Gen. **37**, 9791 (2004).

[9] M. V. Basilevsky and D. Parsons, J. Chem. Phys. **108**, 9107 (1998).

[10] A. Rubinstein and S. Sherman, Biophys. J. **87**, 1544 (2004).

[11] A. A. Kornyshev, A. I. Rubinshtein, and M. A. Vorotyntsev, J. Phys. C **11**, 3307 (1978).

[12] M. Vorotyntsev, J. Phys. C **11**, 3323 (1978).

[13] A. Hildebrandt, R. Blossey, S. Rjasanow, O. Kohlbacher, and H.-P. Lenhof, Phys. Rev. Lett. **93**, 108104 (2004).

[14] J. P. Bardhan, M. G. Knepley, and P. Brune, Mol. Based Math. Biol. **3**, 1 (2015).

[15] D. Xie, Y. Jiang, P. Brune, and L. R. Scott, SIAM J. Sci. Comput. **34**, B107 (2012).

[16] D. Xie, Y. Jiang, and L. R. Scott, SIAM J. Sci. Comput. **38**, B1267 (2013).

[17] D. Xie and Y. Jiang, A nonlocal modified Poisson-Boltzmann equation and finite element solver for computing electrostatics of biomolecules, 2015 (unpublished).

[18] D. Xie and H. Volkmer, Commun. Comput. Phys. **13**, 174 (2013).

[19] J. G. Kirkwood, J. Chem. Phys. **2**, 351 (1934).

[20] D. Xie, J. Comput. Phys. **275**, 294 (2014).

[21] See http://www.poissonboltzmann.org/pdb2pqr/.

[22] See http://www.rcsb.org/.

[23] P. Debye, *Polar Molecules* (Dover, New York, 1945).

[24] D. Griffiths, *Introduction to Electrodynamics*, 3rd ed. (Prentice Hall, NJ, 1999).

[25] B. Roux and T. Simonson, Biophys. Chem. **78**, 1 (1999).

[26] U. Kaatze, R. Behrends, and R. Pottel, J. Non-Cryst. Solids **305**, 19 (2002).

[27] A. Kornyshev and A. Nitzan, Z. Phys. Chem. **215**, 701 (2001).

[28] A. Hildebrandt, Ph.D. thesis, Saarlandes University, Saarbrücken, Germany, 2005.

[29] L. Evans, *Partial Differential Equations*, Graduate Studies in Mathematics Vol. 19 (American Mathematical Society, Providence, 1998).

[30] See Supplemental Material at http://link.aps.org/supplemental/10.1103/PhysRevE.93.043304 for a short user guide on the usage and free download of the program package.

[31] F. Olver, D. Lozier, R. Boisvert, and C. Clark, *NIST Handbook of Mathematical Functions* (Cambridge University Press, Cambridge, UK, 2010).

[32] F. W. Schäfke, *Einführung in die Theorie der Speziellen Funktionen der Mathematischen Physik* (Springer-Verlag, Berlin, 1963).

[33] E. W. Hobson, *The Theory of Spherical Harmonics and Ellipsoidal Harmonics* (Chelsea Publishing Company, New York, 1931).